

## Hyperpolarizability and Operational Magic Wavelength in an Optical Lattice Clock

R. C. Brown,<sup>1,\*</sup> N. B. Phillips,<sup>1,†</sup> K. Beloy,<sup>1</sup> W. F. McGrew,<sup>1,2</sup> M. Schioppo,<sup>1,‡</sup> R. J. Fasano,<sup>1,2</sup> G. Milani,<sup>1,§</sup> X. Zhang,<sup>1,||</sup> N. Hinkley,<sup>1,2,¶</sup> H. Leopardi,<sup>1,2</sup> T. H. Yoon,<sup>1,¶</sup> D. Nicolodi,<sup>1</sup> T. M. Fortier,<sup>1</sup> and A. D. Ludlow<sup>1,\*\*</sup>

<sup>1</sup>National Institute of Standards and Technology, 325 Broadway, Boulder, Colorado 80305, USA

<sup>2</sup>University of Colorado, Department of Physics, Boulder, Colorado 80309, USA

(Received 10 May 2017; published 19 December 2017)

Optical clocks benefit from tight atomic confinement enabling extended interrogation times as well as Doppler- and recoil-free operation. However, these benefits come at the cost of frequency shifts that, if not properly controlled, may degrade clock accuracy. Numerous theoretical studies have predicted optical lattice clock frequency shifts that scale nonlinearly with trap depth. To experimentally observe and constrain these shifts in an <sup>171</sup>Yb optical lattice clock, we construct a lattice enhancement cavity that exaggerates the light shifts. We observe an atomic temperature that is proportional to the optical trap depth, fundamentally altering the scaling of trap-induced light shifts and simplifying their parametrization. We identify an “operational” magic wavelength where frequency shifts are insensitive to changes in trap depth. These measurements and scaling analysis constitute an essential systematic characterization for clock operation at the 10<sup>-18</sup> level and beyond.

DOI: 10.1103/PhysRevLett.119.253001

Optical dipole trapping has risen from theory [1] to establish itself as a workhorse experimental technique in numerous contexts [2–5]. Despite the fact that dipole trapping is achieved by inducing large light shifts, it has found prominence in quantum metrology and precision measurements. The concept of magic wavelength trapping resolves this apparent contradiction by inducing identical shifts on two atomic states of interest [6]. In an optical clock, the energy difference of these states gives the frequency reference that serves as the time base. The magic wavelength allows optical lattice clocks [7] to realize the unperturbed atomic transition frequency while maintaining the experimental benefits of trapped systems. Magic wavelength trapping has found applications far beyond atomic clocks including: cavity QED [8], ultracold molecules [9] and Rydberg gases [10], atomic qubits [11,12], laser cooling [13], and quantum simulation [14,15].

Magic wavelength optical lattices have enabled optical clocks to achieve unprecedented levels of performance, with fractional frequency instability approaching  $1 \times 10^{-18}$  [16–20] and total systematic uncertainty in the 10<sup>-18</sup> range [17–19]. Consequently, optical clocks become sensitive tools for measuring the gravitational red shift and geopotential [21–24], searching for dark matter [25–27], constraining physics beyond the standard model [28–30], improving very long baseline interferometry [31], and, ultimately, redefining the second [32]. However, at these performance levels, the concept of magic wavelength confinement breaks down [33,34]. Higher-order couplings, including magnetic dipole (*M*1), electric quadrupole (*E*2), and hyperpolarizability, prevent a complete cancellation of the light shifts between clock states, introducing shifts that scale nonlinearly with trap depth.

In an <sup>171</sup>Yb optical lattice clock, we measure nonlinear light shifts, offering improved determinations of the hyperpolarizability and lattice magic frequency  $\nu_{\text{magic}}$  [35–38]. Theoretical studies suggest that these higher-order light shifts yield lattice-band-dependent effects [34,39–41] which vary with atomic temperature, complicating characterization of the light shift and its appropriate extrapolation to zero. In this Letter, we extend the theory and experimentally study these temperature-dependent effects. Doing so reveals a simplification in the shift’s functional form, achieving  $1.2 \times 10^{-18}$  clock shift uncertainty. The nonlinear shifts offer an experimental benefit in the form of “operational magic wavelength” behavior—where the polarizability can be tuned, with laser frequency, to partially compensate the hyperpolarizability and yield linear shift insensitivity to trap depth. These measurements and analysis are relevant for other atomic species, including <sup>87</sup>Sr, where the role of hyperpolarizability for accurate characterization of lattice light shifts differs between studies [18,19,42–45].

The dominant optical trap ac Stark effect is from electric dipole polarizability ( $\alpha_{E1}$ ), giving a shift that scales to leading order with trap depth. The differential shift of the clock transition is eliminated at the magic frequency [33]. Higher multipolarizabilities from magnetic dipole and electric quadrupole contributions (denoted here as  $\alpha_{M1E2}$ ) yield much smaller shifts. The hyperpolarizability ( $\beta$ ) shift accounts for electric dipole effects that are fourth order in the electric field. In general, the frequency shift on the clock transition,  $\delta\nu_{\text{clock}}$ , is

$$\frac{\delta\nu_{\text{clock}}}{\nu_{\text{clock}}} = -U\Delta\alpha'_{E1}X_{\mathbf{n}} - U\Delta\alpha'_{M1E2}Y_{\mathbf{n}} - U^2\Delta\beta'Z_{\mathbf{n}}, \quad (1)$$

where all quantities appearing on the right-hand side are dimensionless [46]. Here,  $\Delta$  denotes a difference in a quantity between clock states, and  $\Delta\alpha'_{E1} = \Delta\alpha_{E1}E_r/\alpha_{E1}(\nu_{\text{magic}})h\nu_{\text{clock}}$ ,  $\Delta\alpha'_{M1E2} = \Delta\alpha_{M1E2}E_r/\alpha_{E1}(\nu_{\text{magic}})h\nu_{\text{clock}}$ ,  $\Delta\beta' = \Delta\beta E_r^2/\alpha_{E1}(\nu_{\text{magic}})^2 h\nu_{\text{clock}}$ .  $X_{\mathbf{n}}$ ,  $Y_{\mathbf{n}}$ , and  $Z_{\mathbf{n}}$  represent expectation values of the spatial portion of the trapping potential,  $\mathcal{U}(z, \rho) = \exp(-2\rho^2/w_0^2)\cos^2(kz)$ , for the motional state  $\mathbf{n}$  with a  $1/e^2$  lattice-beam-intensity radius  $w_0$ ;  $X_{\mathbf{n}} \equiv \langle \mathbf{n} | \mathcal{U}(z, \rho) | \mathbf{n} \rangle$ ,  $Y_{\mathbf{n}} \equiv \langle \mathbf{n} | \mathcal{U}(z + \pi/(2k), \rho) | \mathbf{n} \rangle$ ,  $Z_{\mathbf{n}} \equiv \langle \mathbf{n} | \mathcal{U}(z, \rho)^2 | \mathbf{n} \rangle$ .  $U$ , which is proportional to lattice intensity, is the dimensionless ratio of trap depth to recoil energy  $E_r = (\hbar^2 k^2 / 2m)$ , where  $k = 2\pi\nu_l/c$  for lattice frequency  $\nu_l$ ,  $h = 2\pi\hbar$  is Planck's constant,  $c$  is the speed of light, and  $m$  is the mass of  $^{171}\text{Yb}$ .

Here, we extend the perturbative treatment in the harmonic motional-state basis [41] to consider not only longitudinal confinement along the 1D optical lattice, but also transverse optical confinement. The resulting lattice-induced shift for an atom in longitudinal lattice band  $n_z$  and transverse motional state  $n_\rho = n_x + n_y$  is

$$\begin{aligned} \frac{\delta\nu_{\text{clock}}}{\nu_{\text{clock}}} = & n_5 \Delta\alpha'_{M1E2} + [(n_1 + n_2)\Delta\alpha'_{E1} - n_1 \Delta\alpha'_{M1E2}] U^{\frac{1}{2}} \\ & - [\Delta\alpha'_{E1} + (n_3 + n_4 + 4n_5)\Delta\beta'] U \\ & + [2\Delta\beta'(n_1 + n_2)] U^{\frac{3}{2}} - \Delta\beta' U^2. \end{aligned} \quad (2)$$

This treatment yields a  $U^{1/2}$  scaling originating from  $\alpha_{M1E2}$  [34,39] and a  $U^{3/2}$  scaling originating from  $\beta$  [40] and now includes contributions from both the transverse and longitudinal motional quantum numbers:  $n_1 = (n_z + 1/2)$ ,  $n_2 = [\sqrt{2}/(kw_0)](n_\rho + 1)$ ,  $n_3 = (3/2)(n_z^2 + n_z + 1/2)$ ,  $n_4 = [8/(3k^2 w_0^2)](n_\rho^2 + 2n_\rho + 3/2)$ , and  $n_5 = 1/(\sqrt{2}kw_0) \times (n_z + 1/2)(n_\rho + 1)$ .

Since measurements cannot be made at zero trap depth, extrapolation to the unperturbed clock transition frequency at  $U = 0$  is required. For shallow traps with cold low-density atomic samples, an extrapolation linear in  $U$  has generally been considered sufficient to determine the magic wavelength and unperturbed atomic frequency at the  $10^{-17}$  level of clock uncertainty. However, as the required accuracy increases, the higher order terms in Eq. (2) cannot, in general, be neglected. The added fit parameters from each  $U$ -dependent term place a statistical burden on the measurement in order to reach the desired level of uncertainty. Furthermore, the inclusion of these higher-order terms introduces contributions dependent on the thermally averaged  $\langle n \rangle$ . In order to meaningfully apply Eq. (2) to experimental data, the  $\langle n \rangle$  must be characterized over the range of  $U$  measured.

To experimentally observe light shifts in an  $^{171}\text{Yb}$  optical lattice clock [16], we use a power enhancement cavity (finesse  $\approx 200$  at  $\nu_l$ , transparent at  $\nu_{\text{clock}}$ ) to form the optical lattice, Fig. 1(a), enabling trap depths  $>20\times$  our anticipated

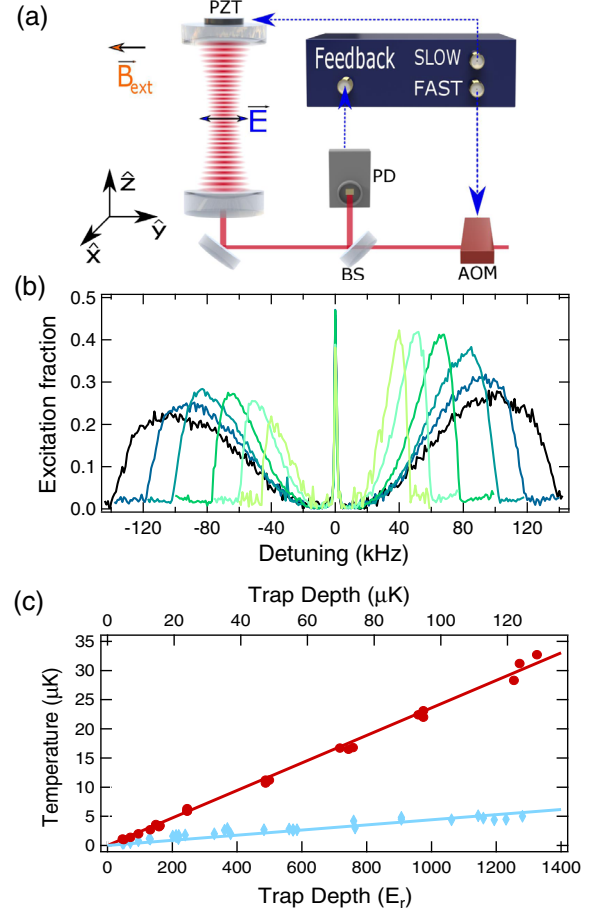


FIG. 1. (a) Schematic of the vertically oriented lattice build up cavity, with out-of-vacuum mirrors. Photodiode (PD), beam-splitter (BS), acousto-optical modulator (AOM), piezoelectric transducer (PZT). (b) Sideband spectra for multiple trap depths from  $150 E_r$  (light green trace) to  $1260 E_r$  (black trace), shown as the measured excited state ( $^3P_0$ ) fraction versus laser detuning from the  $^1S_0$ - $^3P_0$  clock transition frequency (c) Longitudinal temperatures, which characterize the Boltzmann distribution of atomic population among the lattice bands, are extracted from sideband spectra over a range of trap depths. The red trace corresponds to normal operating conditions, while the blue trace incorporates additional sideband cooling.

operational depth [42]. A relatively large lattice beam radius ( $170 \mu\text{m}$ ) in the transverse plane enables a high trapped atom number with relatively low atomic density and, thus, small density-dependent collisional shifts. The cavity orientation along gravity suppresses resonant tunneling between lattice sites [50,51]. To ensure that the optical lattice has no significant residual circular polarization (e.g., vacuum window birefringence), the difference frequency between  $\pi$  transitions from both  $m_F = \pm 1/2$  [52] states is measured for all  $U$ . Residual circular polarization would cause a  $U$ -dependent vector ac Stark shift in the observed splitting. No such dependence is observed, allowing us to constrain lattice ellipticity below 0.6%. Using the vector ac Stark splitting as an *in situ* atomic sensor of optical lattice polarization allows

us to exclude polarization-dependent variations in the observed hyperpolarizability effect [36]. The lattice laser frequency is stabilized to a cavity with a typical drift of  $\lesssim 100$  kHz per day. The absolute lattice laser frequency was measured to within  $\approx 10$  kHz using a referenced Ti:sapphire optical frequency comb [53,54].

Atomic temperature in the transverse and longitudinal lattice dimensions, as well as the magnitude of  $U$ , is assessed for all clock shift measurements via motional sideband spectroscopy, Fig. 1(b) [55]. We observe that the temperature scales predominantly linear in  $U$ , Fig. 1(c). We attribute this linear scaling to the interplay of lattice induced light shifts on the  $^1S_0 \rightarrow ^3P_1$  cooling transition and the atomic kinetic energy cutoff imposed by the finite  $U$ . The linear scaling of temperature with  $U$  has important consequences: for our observed ratio of temperature to trap depth, the following lowest-order approximations hold:  $\langle n_1 \rangle, \langle n_2 \rangle \propto \sqrt{U}$  and  $\langle n_3 \rangle, \langle n_4 \rangle, \langle n_5 \rangle \propto U$ . Under these conditions, Eq. (2) can be reduced to

$$\delta\nu_{\text{clock}}/\nu_{\text{clock}} = -\alpha^*U - \beta^*U^2, \quad (3)$$

with  $U$ -independent finite-temperature polarizabilities  $\alpha^*$  and  $\beta^*$  [46].

Intensity dependent light shifts were measured with interleaved comparisons of the frequency shift between test- and reference-lattice depth clock configurations, as in Ref. [36]. The density shift was independently measured as a function of trap depth to apply small ( $< 4 \times 10^{-18}$ ) corrections to the measured light-shift data, minimally impacting the value of  $\nu_{\text{zero}}$ . For a given lattice frequency, clock shifts were measured as a function of trap depth, Fig. 2(a). Each color represents data sets with a distinct  $\nu_l$ . The uncertainties in  $\delta\nu_{\text{clock}}/\nu_{\text{clock}}$  are the total Allan deviation at the end of each data run ( $\approx 1 \times 10^{-17}$ ).

We analyze the experimental data in Fig. 2(a) by fitting each data set to a modified form of Eq. (3) (plus a constant term to account for the  $U \neq 0$  reference condition). In principle, a fit with a single quadratic coefficient could be justified because hyperpolarizability has negligible lattice frequency dependence in the vicinity of the magic wavelength. Nevertheless, it is possible for  $\Delta\alpha_{E1}$  effects to couple to  $\beta^*$ , giving it dependence on lattice frequency. This situation can arise, for example, from atomic temperature that scales nonlinear in the trap depth. Therefore, we perform fits with and without a global  $\beta^*$ , with both methods yielding a mean value of  $\beta^* = -5.5(2) \times 10^{-22}$  [56].  $\beta^* < \Delta\beta'$  due to the finite temperature of the system; atoms in higher motional states are more spatially delocalized and, thus, experience lower average lattice laser intensity. Nonlinear scaling of the atomic temperature can have other important consequences, such as light shifts with additional  $U$  dependencies that must be included in Eq. (3) for high accuracy shift determination. Because we have observed a residual quadratic dependence of the

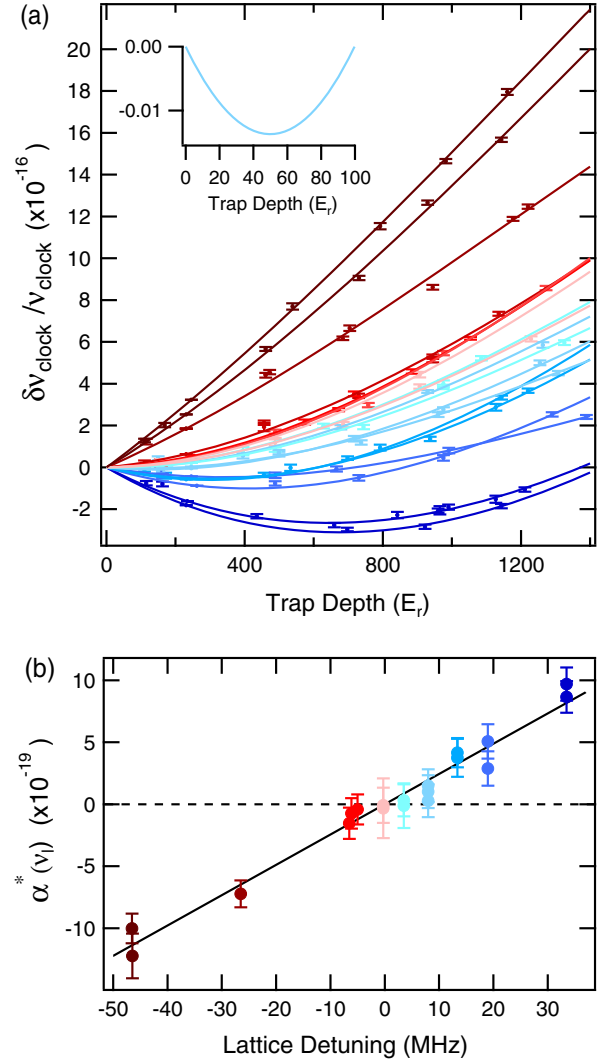


FIG. 2. (a) Clock shifts as a function of lattice depth. Colored traces represent data sets with distinct detunings of  $\nu_l$  from  $\nu_{\text{zero}}$  from  $\approx -50$  MHz (dark red) to  $\approx 30$  MHz (dark blue). This color scheme is quantified in Fig. 2(b). Inset: At the operational magic wavelength for a  $50 E_r$  lattice depth, a 10% change in trap depth creates a  $1 \times 10^{-19}$  change in  $\delta\nu_{\text{clock}}/\nu_{\text{clock}}$ . (b) Linear coefficients from the global fit, primarily proportional to  $\Delta\alpha_{E1}$ , as a function of lattice laser detuning from  $\nu_{\text{zero}}$ . The data are corrected for measured density shifts but not for calculated  $M1/E2$  effects.

transverse atomic temperature versus trap depth, we also allow for a  $U^3$ -dependent fit term [46]. The linear coefficients,  $\alpha^*$ , extracted from the fits to data in Fig. 2(a), are shown in Fig. 2(b). These coefficients scale linearly with the lattice detuning and are parametrized as  $\alpha^*(\nu_l) = (\partial\alpha^*/\partial\nu_l) \times (\nu_l - \nu_{\text{zero}})$ . Fitting to this functional form, we find  $\partial\alpha^*/\partial\nu_l = 2.46(10) \times 10^{-20}$  (1/MHz) and that the linear shift vanishes at  $\nu_{\text{zero}} = 394\,798\,267(1)$  MHz. Using a second independent atomic system with similar experimental conditions, we observe consistent values of  $\partial\alpha^*/\partial\nu_l$ ,  $\beta^*$ , and  $\nu_{\text{zero}}$  between the two systems. For anticipated clock operation with a trap depth of  $50 E_r$ ,

our determinations of  $\alpha^*$  and  $\beta^*$  are sufficient for  $10^{-18}$  uncertainty.

By inspection of Eq. (2), and with  $\langle n_1 \rangle, \langle n_2 \rangle \propto \sqrt{U}$  and  $\langle n_5 \rangle \propto U$ , we see that both  $E1$  and  $M1/E2$  frequency shifts scale linearly with  $U$ . Thus, the dominant effect of  $M1/E2$  contributions is to move the observed zero value of the linear shift away from the lattice frequency where  $\Delta\alpha_{E1} = 0$ ,  $\nu_{\text{zero}} = \nu_{\text{magic}} - \nu_{M1E2}$ . To estimate the effect, we perform a configuration interaction plus many-body perturbation theory calculation [57] and determine  $\Delta\alpha'_{M1E2} = 4(4) \times 10^{-8} (E_r/h\nu_{\text{clock}})$  corresponding to  $\nu_{M1E2} \approx -400$  kHz. This result follows from the partial cancellation of larger terms, yielding a large relative uncertainty. Although  $\nu_{\text{magic}}$  can be deduced from our experimentally measured  $\nu_{\text{zero}}$  and theoretically calculated  $\nu_{M1E2}$ , we emphasize that  $\nu_{\text{zero}}$  represents an experimentally relevant quantity to zero all linear shifts in Eq. (3).

To highlight the role of atomic temperature, we measure lattice light shifts under two distinct thermal conditions. Figure 3 displays the light shift versus trap depth with and without an additional stage of quenched sideband cooling along the lattice axis on the ultranarrow  $^1S_0 \rightarrow ^3P_0$  clock transition [37,58]. As seen in Fig. 1(c), the sideband cooling reduces the longitudinal temperature by a factor of  $\geq 6$ , ranging from just 400 nK to 5  $\mu$ K and with a predominantly linear dependence on  $U$ . In Fig. 3, the observed shifts are larger in the cooled case, since the near-unity population in the ground lattice band experiences the highest lattice laser intensity. The measured hyperpolarizability effect in the sideband-cooled case increases  $\beta^*$  by 12(5)%. This change in  $\beta^*$  introduced by cooling just one dimension underscores the importance of characterizing thermal effects on lattice shifts.

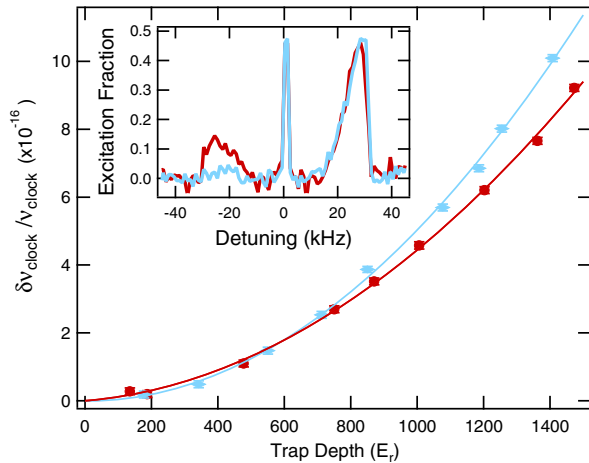


FIG. 3. To experimentally explore the role of finite temperature effects, we measure  $\delta\nu_{\text{clock}}/\nu_{\text{clock}}$  near  $\nu_{\text{zero}}$  both with (blue data) and without (red data) sideband cooling. Cooler atoms are more localized in the high-intensity portion of the lattice; thus, they experience a larger hyperpolarizability shift. The inset shows representative sideband traces.

Using the preceding expressions and taking into account thermal effects, we translate the measured  $\beta^*$  and  $\alpha^*$  to the respective atomic properties  $\Delta\beta' \approx -10 \times 10^{-22}$  and  $\partial\Delta\alpha'_{E1}/\partial\nu_l \approx 4 \times 10^{-20} (1/\text{MHz})$ . Alternatively, known lifetime and polarizability data can be used to calculate  $\partial\Delta\alpha'_{E1}/\partial\nu_l = 4.5(3) \times 10^{-20} (1/\text{MHz})$ . While agreement between theory and experiment is reassuring, the perturbative treatment does not fully account for anharmonic and cross-dimensional effects relevant for higher-lying motional states. We have developed more sophisticated models for evaluating Eq. (1) accounting for these effects [59]. Importantly, we find a key behavior is maintained in more refined analyses: given a linear relationship between temperature and depth, the clock shift is well approximated by Eq. (3) with  $\alpha^*$  and  $\beta^*$  being independent of depth.

The fitted parameters enable us to identify a  $U$ -dependent operational magic frequency. Neglecting any residual  $U^3$  shift dependence or  $\beta^*$  detuning dependence,  $\nu_{\text{opmagic}} \equiv (-2\beta^*U)/(\partial\alpha^*/\partial\nu_l) + \nu_{\text{zero}}$ . At this value of  $\nu_l$  and corresponding  $U$ , a negative linear light shift partially cancels the positive hyperpolarizability shift, yielding a shift with first-order insensitivity to fluctuations in  $U$ . Solving for a trap depth at 50  $E_r$ , the measurements in Fig. 2 indicate an operational magic wavelength of 2.2(1) MHz above  $\nu_{\text{zero}}$ . Although typically controlled at the 1% level, a 10% change in trap depth creates a  $< 1 \times 10^{-19}$  change in  $\delta\nu_{\text{clock}}/\nu_{\text{clock}}$ . This parameter regime is shown as an inset in Fig. 2(a).

While the combination of hyperpolarizability and lattice detuning are useful for achieving operational magic wavelengths, they can also obscure determination of  $\nu_{\text{zero}}$  and  $\nu_{\text{clock}}$  when deduced from measurements experimentally limited to a restricted range of  $U$ . In the simplest case, one can mistake a local minimum for a flat line leading to extrapolation errors in  $\nu_{\text{clock}}$  and incorrect determinations of  $\nu_{\text{zero}}$ . Consider our measured parameters [ $\beta^* = -5.5(2) \times 10^{-22}$ ,  $\partial\alpha^*/\partial\nu_l = 2.46(10) \times 10^{-20} (1/\text{MHz})$ ] and experimental shift uncertainties  $\pm 1 \times 10^{-17}$ . For a measurement range limited from 100 to 300  $E_r$ , variation of lattice light shifts would be  $< 6 \times 10^{-18}$  at a detuning of 8.9 MHz from  $\nu_{\text{zero}}$  (the operational magic wavelength for the middle of the measurement interval: 200  $E_r$ ). At this detuning, the clock shift would appear independent of  $U$ , giving the illusion of magic wavelength operation and making it statistically challenging to resolve hyperpolarizability or nonmagic linear shifts [60]. Linearly extrapolating to  $U = 0$ , errors in  $\delta\nu_{\text{clock}}/\nu_{\text{clock}}$  of  $2 \times 10^{-17}$  and a corresponding error in  $\nu_{\text{zero}}$  of 8.9 MHz could result. Such a difficulty in resolving hyperpolarizability and the resulting error in the light shift determination is general for all lattice laser frequencies (not restricted to  $\nu_{\text{opmagic}}$ ) and may apply to other atomic species. The case of  $^{87}\text{Sr}$  is notable, due to previous measurements and disagreement about the role of hyperpolarizability [18,19,42–45]. While the scaling of

atomic temperature with trap depth has not been fully considered, experimental parameters have been reported for strontium [ $\Delta\beta' = -10(3) \times 10^{-22}$  [44],  $\Delta\beta' = -7(7) \times 10^{-22}$  [19], and  $\partial\Delta\alpha'_{E1}/\partial\nu_l = 3.6(3) \times 10^{-20}$  (1/MHz) [61]]. A similar analysis to that above finds linear versus nonlinear extrapolations over the same limited range of  $U$  leads to differences in the shift determination  $\delta\nu_{\text{clock}}/\nu_{\text{clock}}$  up to  $(2-4) \times 10^{-17}$ . It seems that the role of nonlinear extrapolations in  $^{87}\text{Sr}$  will hinge on developing consensus on the magnitude of  $\beta^*$ , including proper accounting of the temperature scaling with  $U$ . Furthermore, this consideration can guide ongoing work in Mg [62], Hg [63], and Cd [64].

In conclusion, we have precisely characterized optical lattice induced light shifts including nonlinear hyperpolarizability effects. Our measurements highlight the importance of finite temperature effects at  $10^{-18}$  fractional frequency accuracy. We have also experimentally demonstrated a metrologically useful regime, the operational magic wavelength, where changes in light shifts can be minimized as the trap depth changes. Furthermore, by implementing quenched sideband cooling along the 1D lattice axis, tunneling related shifts are suppressed, while somewhat warmer transverse temperatures reduce overall lattice light shifts. These measurements further lay the framework for controlling lattice light shifts at the  $10^{-19}$  level.

This work was supported by NIST, NASA Fundamental Physics, and DARPA QuASAR. R. C. B. acknowledges support from the NRC RAP. We appreciate absolute frequency comb measurements by F. Quinlan, useful discussions with C. Oates, D. Hume, and G. Hoth, and technical assistance from J. Sherman.

Contributions to this article by workers at NIST, an agency of the U.S. Government, are not subject to U.S. copyright. R. C. B. and N. B. P. contributed equally to this work.

\*Present address: Georgia Tech Research Institute, Atlanta, GA 30332, USA; brown171@gatech.edu

†Present address: Stable Laser Systems, Boulder, Colorado, USA.

‡Present address: National Physical Laboratory (NPL), Teddington, TW11 0LW, United Kingdom.

§Permanent address: Istituto Nazionale di Ricerca Metrologica, Strada delle Cacce 91, 10135 Torino, Italy; Politecnico di Torino, Corso duca degli Abruzzi 24, 10125 Torino, Italy.

||Permanent address: State Key Laboratory of Advanced Optical Communication Systems and Networks, Institute of Quantum Electronics, School of Electronics Engineering and Computer Science, Peking University, Beijing 100871, China.

¶Permanent address: Department of Physics, Korea University, 145 Anam-ro, Seongbuk-gu, Seoul 02841, South Korea.

\*\*andrew.ludlow@nist.gov

- [1] V. S. Letokhov, Pis'ma Zh. Eksp. Teor. Fiz. **7**, 348 (1968); [JETP Lett. **7**, 272 (1968)].
- [2] R. Grimm, M. Weidemüller, and Y. B. Ovchinnikov, *Adv. At. Mol. Opt. Phys.* **42**, 95 (2000).
- [3] I. Bloch, J. Dalibard, and W. Zwerger, *Rev. Mod. Phys.* **80**, 885 (2008).
- [4] H. J. Kimble, *Nature (London)* **453**, 1023 (2008).
- [5] Y. O. Dudin, A. G. Radnaev, R. Zhao, J. Z. Blumoff, T. A. B. Kennedy, and A. Kuzmich, *Phys. Rev. Lett.* **105**, 260502 (2010).
- [6] J. Ye, H. Kimble, and H. Katori, *Science* **320**, 1734 (2008).
- [7] M. Takamoto, F.-L. Hong, R. Higashi, and H. Katori, *Nature (London)* **435**, 321 (2005).
- [8] J. McKeever, J. R. Buck, A. D. Boozer, A. Kuzmich, H.-C. Nägerl, D. M. Stamper-Kurn, and H. J. Kimble, *Phys. Rev. Lett.* **90**, 133602 (2003).
- [9] J. G. Danzl, M. J. Mark, E. Haller, M. Gustavsson, R. Hart, J. Aldegunde, J. M. Hutson, and H.-C. Nägerl, *Nat. Phys.* **6**, 265 (2010).
- [10] E. A. Goldschmidt, D. G. Norris, S. B. Koller, R. Wyllie, R. C. Brown, J. V. Porto, U. I. Safronova, and M. S. Safronova, *Phys. Rev. A* **91**, 032518 (2015).
- [11] N. Lundblad, M. Schlosser, and J. V. Porto, *Phys. Rev. A* **81**, 031611 (2010).
- [12] J. Yang, X. He, R. Guo, P. Xu, K. Wang, C. Sheng, M. Liu, J. Wang, A. Derevianko, and M. Zhan, *Phys. Rev. Lett.* **117**, 123201 (2016).
- [13] P. M. Duarte, R. A. Hart, J. M. Hitchcock, T. A. Corcovilos, T.-L. Yang, A. Reed, and R. G. Hulet, *Phys. Rev. A* **84**, 061406 (2011).
- [14] F. Scazza, C. Hofrichter, M. Höfer, P. De Groot, I. Bloch, and S. Fölling, *Nat. Phys.* **10**, 779 (2014).
- [15] G. Cappellini, M. Mancini, G. Pagano, P. Lombardi, L. Livi, M. S. De Cumis, P. Cancio, M. Pizzocaro, D. Calonico, F. Levi *et al.*, *Phys. Rev. Lett.* **113**, 120402 (2014).
- [16] N. Hinkley, J. A. Sherman, N. B. Phillips, M. Schioppo, N. D. Lemke, K. Beloy, M. Pizzocaro, C. W. Oates, and A. D. Ludlow, *Science* **341**, 1215 (2013).
- [17] B. Bloom, T. Nicholson, J. Williams, S. Campbell, M. Bishof, X. Zhang, W. Zhang, S. Bromley, and J. Ye, *Nature (London)* **506**, 71 (2014).
- [18] I. Ushijima, M. Takamoto, M. Das, T. Ohkubo, and H. Katori, *Nat. Photonics* **9**, 185 (2015).
- [19] T. Nicholson, S. Campbell, R. Hutson, G. Marti, B. Bloom, R. McNally, W. Zhang, M. Barrett, M. Safronova, G. Strouse *et al.*, *Nat. Commun.* **6**, 6896 (2015).
- [20] M. Schioppo, R. C. Brown, W. F. McGrew, N. Hinkley, R. J. Fasano, K. Beloy, T. H. Yoon, G. Milani, D. Nicolodi, J. A. Sherman *et al.*, *Nat. Photonics* **11**, 48 (2017).
- [21] N. Ashby, P. L. Bender, J. L. Hall, J. Ye, S. A. Diddams, S. R. Jefferts, N. Newbury, C. Oates, R. Dolesi, S. Vitale *et al.*, *Proc. Int. Astron. Union* **5**, 414 (2009).
- [22] S. Schiller, G. Tino, P. Gill, C. Salomon, U. Sterr, E. Peik, A. Nevsky, A. Görlitz, D. Svehla, G. Ferrari *et al.*, *Exp. Astron.* **23**, 573 (2009).
- [23] C.-W. Chou, D. Hume, T. Rosenband, and D. Wineland, *Science* **329**, 1630 (2010).
- [24] T. Takano, M. Takamoto, I. Ushijima, N. Ohmae, T. Akatsuka, A. Yamaguchi, Y. Kuroishi, H. Munekane, B. Miyahara, and H. Katori, *Nat. Photonics* **10**, 662 (2016).

- [25] A. Derevianko and M. Pospelov, *Nat. Phys.* **10**, 933 (2014).
- [26] A. Arvanitaki, J. Huang, and K. Van Tilburg, *Phys. Rev. D* **91**, 015015 (2015).
- [27] P. Wcisło, P. Morzyński, M. Bober, A. Cygan, D. Lisak, R. Ciuryło, and M. Zawada, *Nature Astron.* **1**, 0009 (2016).
- [28] N. Huntemann, B. Lipphardt, C. Tamm, V. Gerginov, S. Weyers, and E. Peik, *Phys. Rev. Lett.* **113**, 210802 (2014).
- [29] C. Delaunay and Y. Soreq, [arXiv:1602.04838](https://arxiv.org/abs/1602.04838).
- [30] C. Frugiuele, E. Fuchs, G. Perez, and M. Schlaffer, *Phys. Rev. D* **96**, 015011 (2017).
- [31] D. Normile and D. Clery, *Science* **333**, 1820 (2011).
- [32] F. Riehle, *C. R. Phys.* **16**, 506 (2015).
- [33] H. Katori, M. Takamoto, V. G. Pal'chikov, and V. D. Ovsiannikov, *Phys. Rev. Lett.* **91**, 173005 (2003).
- [34] A. V. Taichenachev, V. I. Yudin, V. D. Ovsiannikov, V. G. Pal'chikov, and C. W. Oates, *Phys. Rev. Lett.* **101**, 193601 (2008).
- [35] Z. W. Barber, J. E. Stalnaker, N. D. Lemke, N. Poli, C. W. Oates, T. M. Fortier, S. A. Diddams, L. Hollberg, C. W. Hoyt, A. V. Taichenachev *et al.*, *Phys. Rev. Lett.* **100**, 103002 (2008).
- [36] N. D. Lemke, A. D. Ludlow, Z. W. Barber, T. M. Fortier, S. A. Diddams, Y. Jiang, S. R. Jefferts, T. P. Heavner, T. E. Parker, and C. W. Oates, *Phys. Rev. Lett.* **103**, 063001 (2009).
- [37] N. Nemitz, T. Ohkubo, M. Takamoto, I. Ushijima, M. Das, N. Ohmae, and H. Katori, *Nat. Photonics* **10**, 258 (2016).
- [38] M. Pizzocaro, P. Thoumany, B. Rauf, F. Bregolin, G. Milani, C. Clivati, G. A. Costanzo, F. Levi, and D. Calonico, *Metrologia* **54**, 102 (2017).
- [39] H. Katori, K. Hashiguchi, E. Y. Il'inova, and V. D. Ovsiannikov, *Phys. Rev. Lett.* **103**, 153004 (2009).
- [40] V. D. Ovsiannikov, V. G. Pal'chikov, A. V. Taichenachev, V. I. Yudin, and H. Katori, *Phys. Rev. A* **88**, 013405 (2013).
- [41] H. Katori, V. D. Ovsiannikov, S. I. Marmo, and V. G. Palchikov, *Phys. Rev. A* **91**, 052503 (2015).
- [42] A. Bruschi, R. Le Targat, X. Baillard, M. Fouché, and P. Lemonde, *Phys. Rev. Lett.* **96**, 103003 (2006).
- [43] P. G. Westergaard, J. Lodewyck, L. Lorini, A. Lecallier, E. A. Burt, M. Zawada, J. Millo, and P. Lemonde, *Phys. Rev. Lett.* **106**, 210801 (2011).
- [44] R. Le Targat, L. Lorini, Y. Le Coq, M. Zawada, J. Guéna, M. Abgrall, M. Gurov, P. Rosenbusch, D. Rovera, B. Nagórny *et al.*, *Nat. Commun.* **4**, 2109 (2013).
- [45] S. Falke, N. Lemke, C. Grebing, B. Lipphardt, S. Weyers, V. Gerginov, N. Huntemann, C. Hagemann, A. Al-Masoudi, S. Häfner *et al.*, *New J. Phys.* **16**, 073023 (2014).
- [46] See Supplemental Material at <http://link.aps.org/supplemental/10.1103/PhysRevLett.119.253001> for further discussion, including Refs. [47–49].
- [47] A. E. Siegman, *Lasers* (University Science Books, Mill Valley, CA, 1986).
- [48] R. Le Targat, L. Lorini, M. Gurov, M. Zawada, R. Gartman, B. Nagórny, P. Lemonde, and J. Lodewyck, in *European Frequency and Time Forum (EFTF), 2012* (IEEE, New York, 2012), pp. 19–22.
- [49] E. A. Cummings, M. S. Hicken, and S. D. Bergeson, *Appl. Opt.* **41**, 7583 (2002).
- [50] The lattice is  $\approx 1.5^\circ$  off of vertical to avoid spurious reflections from view ports.
- [51] P. Lemonde and P. Wolf, *Phys. Rev. A* **72**, 033409 (2005).
- [52] Since  $^{171}\text{Yb}$  has a nuclear spin of  $I = 1/2$ , there is no tensor shift.
- [53] T. M. Fortier, M. S. Kirchner, F. Quinlan, J. Taylor, J. Bergquist, T. Rosenband, N. Lemke, A. Ludlow, Y. Jiang, C. Oates *et al.*, *Nat. Photonics* **5**, 425 (2011).
- [54] T. M. Fortier, A. Bartels, and S. A. Diddams, *Opt. Lett.* **31**, 1011 (2006).
- [55] S. Blatt, J. W. Thomsen, G. K. Campbell, A. D. Ludlow, M. D. Swallows, M. J. Martin, M. M. Boyd, and J. Ye, *Phys. Rev. A* **80**, 052703 (2009).
- [56] For nonlinear fits with  $\chi^2 > 1$ , not all fitting routines by default return the same standard errors. In the case of  $\chi^2 > 1$ , we report uncertainty multiplied by the square root of the reduced  $\chi^2$ .
- [57] V. A. Dzuba and A. Derevianko, *J. Phys. B* **43**, 074011 (2010).
- [58] E. A. Curtis, C. W. Oates, and L. Hollberg, *Phys. Rev. A* **64**, 031403 (2001).
- [59] K. Beloy *et al.* (to be published).
- [60] According to our simulations, an  $F$  test for higher order terms at the 5% level with ten  $10^{-17}$  measurements, would favor the null hypothesis of a lower order fit.
- [61] C. Shi, J.-L. Robyr, U. Eismann, M. Zawada, L. Lorini, R. Le Targat, and J. Lodewyck, *Phys. Rev. A* **92**, 012516 (2015).
- [62] A. P. Kulosa, D. Fim, K. H. Zipfel, S. Rühmann, S. Sauer, N. Jha, K. Gibble, W. Ertmer, E. M. Rasel, M. S. Safronova *et al.*, *Phys. Rev. Lett.* **115**, 240801 (2015).
- [63] R. Tyumenev, M. Favier, S. Bilicki, E. Bookjans, R. L. Targat, J. Lodewyck, D. Nicolodi, Y. L. Coq, M. Abgrall, J. Guna *et al.*, *New J. Phys.* **18**, 113002 (2016).
- [64] Y. Kaneda, J. M. Yarborough, Y. Merzlyak, A. Yamaguchi, K. Hayashida, N. Ohmae, and H. Katori, *Opt. Lett.* **41**, 705 (2016).